Title

Decoding the Long Noncoding RNA During Cardiac Maturation

Journal

Circulation Genomic and Precision Medicine, 9(5)

ISSN

1942-325X

Authors

Touma, Marlin

Kang, Xuedong

Zhao, Yan

et al.

Publication Date

2016-10-01

DOI

10.1161/circgenetics.115.001363

Peer reviewed

HHS Public Access

Author manuscript

Circ Cardiovasc Genet. Author manuscript; available in PMC 2017 October 01.

Published in final edited form as:

Circ Cardiovasc Genet. 2016 October ; 9(5): 395–407. doi:10.1161/CIRCGENETICS.115.001363.

Decoding the Long Noncoding RNA during Cardiac Maturation: A Roadmap for Functional Discovery

Marlin Touma, MD, PhD[1,2], **Xuedong Kang, PhD**[#1], **Yan Zhao, PhD**[#1], **Ashley A. Cass, BS**[3], **Fuying Gao, PhD**[4], **Reshma Biniwale, MD**[5], **Giovanni Coppola, MD**[4], **Xinshu Xiao, PhD**[3], **Brian Reemtsen, MD**[5], and **Yibin Wang, PhD**[2,6]

[1]The Children's Discovery and Innovation Institute (CDI), Department of Pediatrics, University of California, Los Angeles, CA

[2]Cardiovascular Research Laboratory, University of California, Los Angeles, CA

[3]Department of Integrative Biology and Physiology, University of California, Los Angeles, CA

[4]Department of Neurology and Psychiatry, University of California, Los Angeles, CA

[5]Department of Cardiothoracic Surgery, University of California, Los Angeles, CA

[6]Department of Anesthesiology, Physiology and Medicine, University of California, Los Angeles, CA

[#] These authors contributed equally to this work.

Abstract

Background—Cardiac maturation during perinatal transition of heart is critical for functional adaptation to hemodynamic load and nutrient environment. Perturbation in this process has major implications in congenital heart defects (CHDs). Transcriptome programming during perinatal stages is important information but incomplete in current literature, particularly, the expression profiles of the long noncoding RNAs (lncRNAs) are not fully elucidated.

Methods and Results—From comprehensive analysis of transcriptomes derived from neonatal mouse heart left and right ventricles, a total of 45,167 unique transcripts were identified, including 21,916 known and 2,033 novel lncRNAs. Among these lncRNAs, 196 exhibited significant dynamic regulation along maturation process. By implementing parallel weighted gene co-expression network analysis (WGCNA) of mRNA and lncRNA datasets, several lncRNA modules coordinately expressed in a developmental manner similar to protein coding genes, while few lncRNAs revealed chamber specific patterns. Out of 2,262 lncRNAs located within 50 KBs of protein coding genes, 5% significantly correlate with the expression of their neighboring genes. The impact of Ppp1r1b-lncRNA on the corresponding partner gene Tcap was validated in cultured myoblasts. This concordant regulation was also conserved in human infantile hearts. Furthermore,

Correspondence: Marlin Touma, MD, PhD, David Geffen School of Medicine, University of California, Los Angeles, 10833 Le Conte Ave, B2-375, MDCC, Los Angeles, CA 90095, Tel: 310-206-6197, Fax: 310-267-0154, mtouma@mednet.ucla.edu, Yibin Wang, PhD, David Geffen School of Medicine, University of California, Los Angeles, 650 Charles E. Young Dr, BH 569, CHS, Los Angeles, CA 90095, Tel: 310-206-5197, Fax: 310-206-5907, yibinwang@mednet.ucla.edu.

Disclosures: None.

the Ppp1r1b-lncRNA/Tcap expression ratio was identified as a molecular signature that differentiated CHD phenotypes.

Conclusions—The study provides the first high-resolution landscape on neonatal cardiac lncRNAs and reveals their potential interaction with mRNA transcriptome during cardiac maturation. Ppp1r1b-lncRNA was identified as a regulator of Tcap expression with dynamic interaction in postnatal cardiac development and CHDs.

Keywords

congenital cardiac defect; gene regulation; transcriptome; neonatal mouse cardiomyocyte; neonatal heart maturation; LncRNA

Introduction

Perinatal cardiac growth and maturation is critical for functional adaptation of the heart to changes in hemodynamic load, respiration and nutrient environment[1,2]. At birth the adaptation of the cardiovascular system to extra-uterine life, also referred to as perinatal circulatory transition, involves dramatic hemodynamic changes that lead to closure of the fetal shunts, and separation of the pulmonary and the systemic blood flow. Concomitantly, the left and the right ventricles undergo functional modifications and structural remodeling to operate the systemic and the pulmonary circuits, respectively[1,2].

Cardiac development in mammals involves complex cellular differentiation, proliferation, migration and morphogenesis processes, driven by transcriptional network involving key transcription regulators and their perturbations are often causative for congenital heart defects (CHDs)[3-11]. Remarkably, during fetal to neonatal transition period, the vast majority of cardiomyocytes undergo dramatic changes in morphology, function, metabolism, gene expression and proliferative capacity[3-10]. These tightly regulated processes become significantly disrupted in the setting of a preterm birth[1,2] or a congenital heart defect[8, 9,11]. The abnormal physiology of the premature myocardium and the altered anatomy of the impaired heart are further complicated by the persistence of fetal shunt pathways and pathological flow patterns. As such, the growing heart is particularly vulnerable during this critical period to multi-factorial perinatal stresses (sepsis, respiratory failure, surgery) that can consequently lead to significant ventricular dysfunction and circulatory failure.

Transcriptome programming is the driving force for cardiac maturation and functional adaptation during perinatal circulatory transition in normal and pathological conditions. However, although changes in cardiac gene expression have been extensively studied in the developing fetal heart in the postnatal heart[12,13] and in the failing adult heart[14,15], the molecular mechanisms of transcriptome programming in neonatal heart chambers during the critical window of fetal to neonatal maturation remain to be fully revealed. In addition, current stem-cell therapies share a common challenge of cellular immaturity upon differentiation[2,10]. Therefore, understanding the transcriptome landscape during the perinatal window will fill an important gap in cardiac maturation and would have significant implications in CHD and cardiac regeneration.

Recently, the discovery of the long noncoding RNA transcripts (lncRNAs) has expanded the total functional complexity of transcriptome. Featuring temporal regulation, species and tissue specificities and functional diversity[14-19], it is increasingly evident that the lncRNAs play important roles in gene regulation at different levels, including transcription, chromatin modification and post-transcriptional editing[16-28]. The importance of lncRNAs is increasingly recognized in heart development and pathogenesis. Several reports have identified hundreds of lncRNAs enriched in heart, dynamically transcribed during development[18,19,25-27], and differentially regulated in disease[14,18,28,29].

Here, we performed comprehensive analysis of the lncRNAs in neonatal mouse hearts. We found a significant number of these lncRNAs dynamically expressed along postnatal maturation. Further we identified several lncRNA co-expression modules coordinately regulated during postnatal development similar to protein coding genes. Furthermore, we find 5% of the highly regulated lncRNAs significantly correlate with the expression of their corresponding neighboring genes. Finally, we demonstrate that the Ppp1r1b-lncRNA can potently modulate its neighboring partner gene Tcap and the expression ratio of Ppp1r1b-lncRNA/Tcap segregates different types of CHDs. These insights would advance our current understanding of the gene regulatory network and potential disease mechanisms in perinatal heart.

Methods

All animal related experimental protocols were approved by the University of California Los Angeles (UCLA) Animal Care and Use Committee. All human studies were conducted in accordance with regulation of the UCLA-Institutional Review Board (IRB).

Gene expression data have been deposited within the Gene Expression Omnibus (GEO) repository [www.ncbi.nlm.nih.gov/geo] under [Neonatal Heart Maturation (NHM) SupperSeries GSE85728. http://www.ncbi.nlm.nih.gov/geo/query/acc.cgi?acc=GSE85728].

Detailed methods are provided in supplemental information on-line, including: Description of experiments, study design, bioinformatics analysis, WGCNA, network analysis and statistical methods, *in vitro* functional studies, human specimens, molecular validation, primers and GapmeR designs.

RNA-sequencing and bioinformatics analysis

Deep RNA-seq was performed using total RNA isolated from male C57B/6 mouse left ventricle (LV) and right ventricle (RV) at postnatal day 0 (P0, prior to the ductal closure), day 3 (P3, transition), and day 7 (P7, terminal differentiation of the vast majority of cardiomyocytes) (Supplemental Figure 1. A). Strand specific cDNA libraries were constructed from three LV and RV total RNA samples (biological replicates) at each time point with the exception of only two RV samples for day 7. Paired end sequencing reads were aligned to reference mouse genome (UCSDmm9) using TopHat. Reads mapped to reference genome by TopHat were used for assembly. Reference annotation based assembly method wasimplemented to reconstruct the transcripts using Cufflinks to predict novel lncRNAs and using Cuffmerge to merge them.

Identifying known and novel lncRNAs

The constructed transcripts were compared with reference annotation database (NONCODE v4.0) by using Cuffcompare and the known lncRNAs were filtered. The transcripts that do not exist in NONCODE v4.0 database were regarded as candidate novel lncRNAs (Figure 1.A, Supplemental Figure 1.B,C). In order to separate potential protein coding transcripts (PCTs) from putative novel lncRNAs, iSeeRNA software[30], an open reading frame based analyzer capable of defining short ORFs, was used. Finally, further analysis filters that are based on lncRNA definition (transcript length >=200 bp) and features (contains at least one splice junction, given more than 98% of lncRNAs undergo alternative splicing) were performed to identify the novel lncRNAs. Expression levels of the novel and known lncRNAs as well as the mRNAs were estimated using the RPKM measure (reads per Kilobase per million of mapped reads). Cutoff values of 3 RPKM and 0.3 RPKM were used to define significantly expressed mRNA and lncRNA, respectively.

Differential expression analysis

Genes with mean >=3 RPKM and lncRNAs with mean >=1 RPKM in at least one sample (3 biological replicates) of each category and variation (V) >=0.2 across samples were included. Unless otherwise specified, significantly differentially expressed genes/lncRNAs are defined as those with fold change (FC)>=2, at a FDR *P* value <= 0.05.

Weighted gene co-expression network analysis (WGCNA)

Genes with mean RPKM >=3 and lncRNAs with mean RPKM >=0.3 in at least one sample (3 replicates) of each category, and variation >=0.2 across samples were included to construct signed network modules using the R package[31]. The module-trait correlation relationships were calculated (Supplemental Figure 2). Unique stage specific modules were defined as those with correlation coefficient r≥0.7 and *P* value ≤0.005 between the module Eigengene and the maturation stage (P0, P3 or P7).

Genomic position

Known and novel lncRNAs were evaluated if they can be located within 50 KBs upstream or downstream of a protein coding gene by comparing to reference genome. For each lncRNA, all Ensembl genes within the +/− 50kb region that do not overlap with the lncRNA were identified. Requiring no sequence overlaps between the neighboring gene and the lncRNA of interest eliminates the host genes that overlap with a putative lncRNA sequence. The correlation of gene expression for each lncRNA/mRNA pair was calculated using Pearson's correlation and Benjamini-Hochberg (B-H) correction methods. A B-H adjusted correlation *P* value ≤ 0.05 was considered significant.

Human studies

Pediatric patients with clinical diagnosis of teratology of fallot (TOF) or ventricular septum defect (VSD) were enrolled in accordance with regulation of the UCLA-IRB approved protocol. Informed consents were obtained from all participants. Human heart specimens from the right ventricle outflow tract (RVOT) were collected during clinically indicated

cardiac operations. The specimens were immediately snap frozen using liquid nitrogen. Total RNAs were isolated using standard methods.

Statistics

Quantified results are presented as mean±SEM. Comparisons between groups were evaluated using ANOVA or the Student's *t* test; $P \leq 0.05$ was considered significant, unless specified otherwise in supplemental methods.

Results

LncRNAs are Dynamically Regulated in Neonatal Heart Chambers

We implemented deep RNA-sequencing to establish mRNA/lncRNA landscape in neonatal left ventricle (LV) and right ventricle (RV). We obtained tissues from postnatal day 0 (P0, prior to the ductal closure), day 3 (P3, transition), and day 7 (P7, terminal differentiation of the vast majority of cardiomyocytes) (Figure 1. A and Supplemental Figure 1.). Out of the average 30 million paired sequencing reads obtained from each sample, 77% were uniquely mapped to mouse genome and classified according to their categories in reference to UCSDmm10 and NONCODE v4.0. Using cutoff values of 0.3 RPKM and 3 RPKM in at least one sample to define the expressed lncRNAs or mRNAs, respectively, a total of 45,167 unique transcripts were detected, including 21,218 mRNAs and 23,949 lncRNAs. Among the lncRNAs, 2,033 are novel and 21,916 are known (Figure 1. A and Supplemental Figure 1. B,C).

Wide range of lncRNA expression levels in neonatal heart was observed involving known and novel lncRNAs varying from less than 0.1 RPKM for Braveheart and Fendrr, both of which are important for maintaining cardiac fate and differentiation of cardiac progenitors, to ≥ 30 RPKM for the well-known H19 (NONMMUT064276). This wide range of expression is consistent with previous observations in fetal and adult heart[14,18]. Among a total of 23,949 lncRNAs expressed in neonatal heart, 1,286 exhibited significant variation exceeding 0.2 across samples. Among them, 1,099 (863 known and 236 novel) lncRNAs are abundantly expressed (RPKM ≥1), including 242 (214 known and 28 novel) lncRNAs with average RPKM exceeding 3 (Figure 1. B and Supplemental Table 1).

Principal component analysis (PCA) of the top ranked 500 protein coding mRNAs (based on magnitude of changes) across all samples revealed developmental stage as a major contributor to the underlying expression changes (84%) while chamber specificity has a relatively modest role (12%) (Figure 1. C *upper panel)*. Consistent with PCA, unsupervised hierarchical clustering analysis at whole transcriptome level revealed that samples from the same developmental stage clustered together regardless of their chamber identity. Interestingly, transcripts from P3 and P7 clustered relatively close but further away from P0, indicating more robust transcriptome changes during the P0 to P3 window. Furthermore, chamber specific gene expression clusters were identified in P3 and more clearly in P7 hearts, but not in P0, suggesting an increasing level of transcriptome divergence between LV and RV as the heart matures (Figure 1. D *upper panel*).

Similar to mRNAs, the PCA of the top 500 varying lncRNAs (ranked based on magnitude of changes) also revealed that developmental time point is a major source of variation (PC1~85%) (Figure 1. C *lower panel)*. However, chamber based separation was much lower, mainly at P7. Likewise, unsupervised hierarchical clustering on all detected lncRNAs revealed a developmental stage specific lncRNA signature in the neonatal heart without discernable chamber specific differences (Figure 1. D *lower panel*). Similar expression patterns were also revealed by differential expression (DE) analysis that was structured along two schemes: development time points (P0 vs. P3, P3 vs. P7 and P0 vs. P7) and ventricular chamber identity (LV vs. RV) (Figure 2. A). A total of 196 lncRNAs are significantly expressed in at least one maturation window at cut off values of RPKM≥1, V≥0.2, FDR $P \leq 0.05$ and fold change (FC) ≥2 (i.e., log FC≥1), with concordant regulation patterns in both LV and RV (Figure 2. B–D, and Supplemental Table 2). In contrast, NONMMUT054852 was the only differentially expressed lncRNA between LV and RV at FC≥2. Given the chamber specific genes may generally change less than 2 fold, we relaxed the fold-change criterion while tightening the FDR *P* value to ≤0.01. Using these alternate criteria, 16 lncRNAs were identified to be differentially expressed in chamber specific manner, including 5 lncRNAs upregulated in LV and 11 lncRNAs upregulated in RV from at least one time point (Figure 2. E and F, and Supplemental Table 3).

Concordant mRNA/lncRNA Network Modules during Neonatal Heart Maturation

To establish functional relevance of mRNAs and lncRNAs associated with postnatal heart maturation, we performed an unsupervised WGCNA[31] across the three time points. WGCNA on mRNA transcripts (RPKM ≥3, V≥0.2) revealed 18 gene co-expression modules (Figure 3. A). Among them, 8 modules were identified to exhibit significant stage specific expression correlation in both LV and RV (r≥0.7 and $P \leq 0.005$) (Figure 3. B). In total, 2,826 member genes were found in the P0 specific modules (Brown, Blue and Turquoise), comparing to 1,234 genes in the P3 (Light cyan, Salmon and Magenta), and 955 genes in the P7 (Green and Red) modules. Only 2 of the 8 stage specific modules also exhibit chamber specificity. This observation is consistent with the notion that the greatest changes in gene expression in neonatal heart are between P0 and P3, while relatively more gradual changes occur between P3 and P7, and variations in neonatal heart gene expression are predominantly driven by developmental process rather than LV vs. RV differentiation.

From these modules, we identified 155 hub genes based on their intramodular gene connectivity (kME≥0.9 and $P \leq 10^{-10}$). Many of these genes are also identified independently as hub genes in publicly available datasets. For example, Sox4, a hub gene for the Light cyan mRNA module (Figure 3.B), is also consistently identified and verified as a hub gene in separate datasets regulating memory $CD8^+$ T-cell development[32]. Notably, Sox4 has also been implicated in ventricular septation and outflow tract development[33,34]. We also identified a number of hub genes that have not been established in other public datasets providing novel candidates for future mechanistic studies. By carrying out functional enrichment analysis, we found glucose metabolism, cell cycle, chromatin organization and RNA processing enriched in the P0 gene modules, mitochondria, fat metabolism and intracellular organelle formation enriched in P3 gene modules, and signaling, protein synthesis and multicellular organ development enriched in P7 gene modules (Figure 3.C).

Together, these changes reflect step-wise progression in cardiomyocyte differentiation, metabolic maturation and cellular growth during postnatal transition.

When significantly expressed lncRNAs (RPKM ≥0.3, CV ≥0.2) were subjected to parallel gene network analysis using WGCNA, 9 modules were identified (Figure 3. D). Among them, 6 modules are developmental stage specific (Figure 3. E). Similar to the observations made from mRNAs, the developmental stage specific lncRNA modules were largely shared between LV and RV. In contrast, only one lncRNA module (lncRNA-Yellow) exhibits both stage and chamber specific association. In total, 710 lncRNAs were identified in developmental stage specific modules at P0 (Brown, Turquoise and Blue), 152 lncRNAs at P3 (Magenta and Red), and 143 lncRNAs at P7 (Yellow), parallel to the same trends observed for mRNAs in terms of number of changes observed during P0 to P3 window in contrast to P3 to P7 window (Figure 3. E). Remarkably, these stage specific lncRNA modules exhibited reciprocal transition between P0 and P7 during maturation (Figure 3. F).

Notably, 17 lncRNAs were identified to exhibit hub-gene like properties with significant intramedullary connectivity. Of these hub-lncRNAs 11 are members of stage specific modules (Figure 3. E). H19 (NONMMUT064276) was identified as a potential hub gene in the P0-Brown-lncRNA module (Supplemental Figure 4. A and B). We further analyzed potential interaction between lncRNA and mRNA modules by implementing the hypergeometric test for individual modules. A total of 33 lncRNAs (11 known and 22 novel) were identified to be significantly concordant with their corresponding mRNA modules. Notably, more than half of them are members of the P0 lncRNA modules, while 7 of them are from the P7 lncRNA module. Based on their local genomic structure, 11 were identified as natural antisense transcripts (NATs), 19 as sense and 3 as intronic lncRNAs (Supplemental Table 4). Together, these analyses suggest that the overall architectures of the mRNA and the lncRNA transcriptome are largely shared between LV and RV and are likely the product of developmentally regulated transcription programs in neonatal heart.

Functional Implications of LncRNAs

To identify potential regulatory lncRNAs, we focused next on identifying lncRNAs that were located upstream or downstream of an annotated protein coding gene to examine their potential impact on paired neighboring gene expression. The lncRNA/gene pairs were defined as being colocated within 50 kilobases of genomic distance, but with no sequence overlap between the neighboring gene and the lncRNA of interest, thus eliminating the potential lncRNA/host gene pairs. Based on these criteria, a total of 6,996 lncRNA/mRNA pairs were identified on mouse genome. Among them, 2,262 unique lncRNA/gene pairs were detected in neonatal heart (defined as lncRNA-RPKM≥1, mRNA-RPKM≥3, V≥0.2). Of these, 114 lncRNAs, including 12 novel lncRNAs, showed significantly correlated expression pattern with a neighboring mRNA (Pearson's correlation BH-corrected *P* value ≤0.05) during at least one developmental period (Supplemental Table 5). 90.4% of these pairs are positively correlated (e.g., UCP2-lncRNA/UCP3) and 9.6% are negatively correlated (e.g., Ppp1r1b-lncRNA/Tcap) (Figure 4. A and B). By GO analysis of the lncRNA-correlated mRNAs, RNA process (e.g., Hnrnpa1, Sf3b6), cardiac development (e.g., NKX2-5, Hand2), and metabolism (e.g., Luc7l3, UCP3) are top enriched functional

ontology terms. Remarkably, the majority of significantly correlated lncRNA/mRNA pairs are also members of developmental stage-specific lncRNA or mRNA modules with significant correlation with their corresponding module Eigengenes.

LncRNAs are generally poorly conserved across species. However, we find five lncRNAs have conserved ortholog in human, including UCP2-lncRNA (NONMMUT062940), n420212 (NONMMUT041263), Fus-lncRNA (NONMMUT063779), Ppp1r1b-lncRNA (NONMMUT011874) and H19 (NONMMUT064276). Their expressions were detected in infantile heart and altered in different CHDs (Figure 5. a-d and Supplemental Figure 4. C). Importantly, the genomic position and the inverse expression relationship between Fus-lncRNA, or Ppp1r1b-lncRNA with their corresponding neighboring genes Trim72 or Tcap (Figure 5. C and D), respectively, were also highly conserved in human infantile hearts (Figure 5. c and d). Similarly, the genomic position relationships and concordant expression patterns of n420212/KCNB1 and UCP2-lncRNA/UCP3 pairs (Figure 5. A and B) were also conserved in human postnatal heart (Figure 5. a and b). Together, these data suggest that some cardiac lncRNA/mRNA pairs discovered in mouse are also preserved in human.

To validate regulatory relationship of the identified lncRNA/mRNA pairs, we investigated the Ppp1r1b-lncRNA/Tcap pair further. As shown in Figure 5.D, the Ppp1r1b-lncRNA/Tcap mRNA pair exhibit tightly correlated dynamic expression during neonatal heart maturation. In addition, they both are members of the inversely related lncRNA/mRNA modules. While Ppp1r1b-lncRNA significantly correlates with P0-lncRNA-Brown module Eigengene, Tcap is a member of the P7-mRNA-Green module in neonatal mouse heart (Supplemental Figure 5. B and C). Tcap encodes Titin Cap, a muscle specific protein involved in cardiomyocyte sarcomere organization and myogenesis by anchoring Titin filaments at the Z disk[35,36].

As illustrated in Figure 6. A and Figure 8. A, the Ppp1r1b-lncRNA is positioned within 28 KBs upstream of the Tcap gene on mouse chromosome 11, and similarly positioned on human chromosome 17. The Ppp1r1b-lncRNA consists of partial exonic and intronic segments from its host gene Ppp1r1b, as well as a non-overlapping exon fragment that we targeted using GapmeR (Figure 6. A and Supplemental Figure 6). A short open reading frame is identified in the mouse Ppp1r1b-lncRNA, but is predicted to be non-functional. Consistent with qRT-PCR validated expression time course in neonatal mouse heart (Figure 6. B. I,II), the expression time course of Ppp1r1b-lncRNA and Tcap in differentiating C2C12 revealed reciprocal relationship (Figure 6. C. I,II).

In response to Ppp1r1b-lncRNA inhibition in myoblasts, myocyte maturation as measured by myotubes fusion index was blocked by Ppp1r1b-lncRNA inactivation (Figure 7. A, B). Furthermore, significant upregulation of Tcap-mRNA and protein abundance was observed in differentiating myotubes, supporting negative regulatory relationship (Figure 7. C, D) along with suppressed expression of other myogenesis genes[37], including Myom2, and Myoz2 (Figure 7. E). Notably, Ppp1r1b-lncRNA inhibition did not impact the host gene expression, nor other nearby genes (e.g., Stard3-mRNA was not affected). Moreover, the inverse correlation relationship was preserved in GapmeR targeted neonatal cardiomyocytes (Figure 7. F). These data support that the putative Ppp1r1b-lncRNA transcript is not another splice product of the host gene.

More interestingly, both PPP1R1B-lncRNA and the corresponding partner gene TCAP were found to be tightly and inversely co-regulated in human infantile hearts with Tetralogy of Fallot (TOF) with age ranging from 2 to 12 months old (Figure 8. B). Importantly, the negatively correlated relationship between PPP1R1B-lncRNA and TCAP expression was also observed in infant hearts with TOF or VSD (Ventricular Septal Defect) (Figure 8. C). Moreover, the ratio of PPP1R1B-lncRNA and TCAP expression significantly segregated the two types of CHDs (Figure 8. D).

Discussion

Here we performed in-depth characterization of the expressional landscape of lncRNAs relative to mRNAs and revealed interactions among lncRNAs as well as between lncRNA and mRNA gene networks. We find the majority of lncRNAs exhibit developmental stage specific regulation, parallel with mRNA expression patterns. We also observed concordant dynamic regulation of lncRNAs more evident during postnatal heart development than in postnatal chamber specification. Furthermore, we identified novel lncRNA/mRNA pairs implying potentially important roles of lncRNAs in neonatal cardiomyocyte maturation.

The RNA profiling reported in this study complements two recent reports where RNA-seq analyses were performed in postnatal hearts at specific time points, focusing on data from P2 and P13 hearts [12], and from P1 and P21 hearts[13], respectively. However, our current analysis focuses on lncRNA profile and correlation with mRNA in neonatal hearts during the critical window of perinatal circulatory transition (before and after the ductal closure), which was not included in these two datasets. We include more description on the different times during the critical window of perinatal circulatory transition (before and after the ductal closure). We also employ methods different from these two studies. To our knowledge, this is the first time the neonatal heart gene and lncRNA expression profiles have been systematically analyzed in spatial-temporal manner, providing a high-resolution profile of their signature and characteristics during critical fetal to neonatal transition, all of which may help identify important lncRNAs of potential regulatory function impacting neonatal heart maturation and disease.

Our data revealed 1099 lncRNAs abundantly expressed and varied in neonatal heart chambers. Gene network analysis identified coordinated lncRNA and mRNA modules that were shared in a developmental stage specific fashion. Remarkably, sharp changes of the transcriptome complex, including mRNA and lncRNA networks, occurred during P0 to P3 maturation window, likely reflecting the rapid adaptation of cardiovascular system to dramatic changes in circulation, nutrient environment and cellular respiration. These changes impact cardiomyocyte energy demands and metabolism as well as regeneration and functional properties.

A recent report[18] investigated cardiac specific lncRNAs in contrast to liver and skin lncRNAs and identified 117 heart enriched and 104 adult cardiomyocyte enriched lncRNAs (RPKM>=0.3) in mice. Out of these previously reported cardiac lncRNAs, we identified 27 cardiac enriched and 35 adult cardiomyocyte enriched lncRNAs that were expressed in neonatal heart exhibiting dynamic regulation during maturation (Supplemental Table 6).

Remarkably, our findings agree with their report that genomic position of the lncRNAs and their correlated expression with neighboring genes is an important predictor of putative functionality. Therefore, we further compared their differential expression results with our results revealed by combined differential expression and WGCNA analyses. Particularly, all cardiomyocyte and cardiac enriched lncRNAs that are found to be abundantly expressed in our samples (RPKM≥1) revealed stage specific module membership in neonatal heart (Supplemental Figure 7). In addition to the validated cardiac enriched lncRNA/mRNA pair n420212 (NONMMUT041263)/Kcnb1 mRNA, we found other previously validated pairs such as n411949 (NONMMUT042600)/Mccc1 and n413445 (NONMMUT042600)/Relb displaying similar correlated expression in our study. These observations suggest cardiac specific and highly abundant lncRNAs are also highly correlated and connected to their developmental module network, implicating potential functionality in coordinated gene regulation.

A major finding of this study is that lncRNAs exhibit tight temporal regulation during fetal to neonatal maturation and may have important regulatory function during this window. In particular, we identified potential novel regulatory interactions between correlated lncRNAs and neighboring mRNAs in neonatal heart. Tcap encodes a cardiomyocyte specific protein involved in cardiac myogenesis. Trim72 is enriched in heart and regulates sarcolemma response to oxidative stress[38]. The inverse relationship between Ppp1r1b-lncRNA and its neighboring partner gene Tcap and between Fus-lncRNA and Trim72 in neonatal heart suggests potential role of these lncRNAs in cardiomyocyte maturation and early adaptation to postnatal stress. Indeed, our functional studies have demonstrated significant functional impact of Ppp1r1b-lncRNA inactivation on myogenesis and sarcomere assembly by blocking differentiation of C2C12 cells. Additionally, the induction of UCP2-lncRNA and associated UCP3 mRNA may be important for metabolic switch during postnatal myocardium maturation. Together, our findings are of direct clinical value to further understand neonatal heart programming not only during normal maturation, but also during pathological maturation, especially in the context of prematurity and CHDs when metabolic substrates are altered, fetal shunts are often persistent and fetal to neonatal adaptation is delayed or disrupted leading to cardiac and circulatory failure early after birth.

Importantly, some of the mouse neonatal heart lncRNAs have conserved counterparts in human infant hearts with CHDs, and some of the lncRNA/mRNA pairs observed in mouse are also preserved in human. Indeed, the emerging links between lncRNAs and heart development[16,19,23-25] indicate that lncRNAs contribute to core transcriptional regulatory circuits involving key transcription factors that underlie human CHDs[25,4-11]. Our findings showcase that specific lncRNA/mRNA pairs can not only have a significant impact on cellular morphology and function but also be valuable to segregate diseases. In particular, we identified Ppp1r1b-lncRNA/Tcap expression ratio as a molecular signature that differentiated TOF and VSD in human infantile hearts. Therefore, comprehensive profiling of lncRNAs may yield novel biomarkers and therapeutic targets for CHDs and pediatric heart diseases.

Important limitations of our study remain. We used whole ventricle tissue for RNA-seq analysis without first sorting or purifying different cell types. Therefore, the low overall

expression levels of certain lncRNAs may mask the high-level and important expression of these lncRNAs in specific subset of cardiac cells. In addition, future studies using RNA-seq should include more replicates[39]. Furthermore, there are significant deficiencies in the current algorithms for lncRNA identification, and some of these currently annotated lncRNAs may produce micro-peptides as shown by Nelson BR et al.[40,41].

Notably, we observed that vast majority of the lncRNAs that exhibited concordant regulation with protein coding genes are particularly localized within 2 KB distance of their neighboring genes, suggesting a potential *cis* regulatory mechanism of function. However, we recognize that the neighboring gene-pair based analysis is very limited to identify potentially functional lncRNAs since it will miss many long-range trans-acting lncRNAs with their targets, at either transcriptional or post-transcriptional levels. Further, some NATs exhibited significant overlap with concordant lncRNA-mRNA modules, suggesting that at least some lncRNAs also act in *trans* manner, potentially via recruitment of chromatin remodeling complexes. Importantly, we acknowledge that finding obtained from our C2C12 model system may not fully recapitulate maturation process of cardiomyocytes. Employing human cardiomyocytes derived from induced pluripotent stem cells will serve as an ideal approach of functional interrogation in future studies.

Together, our study supports putative regulatory role of lncRNAs in transcriptome programming during a critical window of neonatal heart maturation, adaptation and disease. Our observations reinforce the notion that lncRNAs may use diverse molecular mechanisms to regulate their target genes. Additional functional studies will be needed to clarify their diverse mechanisms and biological function during myocardium maturation providing molecular basis for future investigations on congenital heart disease and stem cell therapy.

Supplementary Material

Refer to Web version on PubMed Central for supplementary material.

Acknowledgments

Authors acknowledge Dr. Thomas Vondriska for the critical review of the manuscript. Authors acknowledge the support of the NINDS Informatics Center at UCLA.

Sources of Funding: This work was supported by grants from National Institutes of Health (NIH)/ Child Health Research Center (5K12HD034610/K12) and the UCLA-Children's Discovery Institute and Today and Tomorrow Children's Fund for Marlin Touma; NIH/Predoctoral training grant (T90DE022734) for Ashley A. Cass; R01HG006264 for Xinshu Xiao; HL070079, HL103205, HL108186 and HL110667, and UCLA-CTSI-Cardiovascular Pilot Team Research Grant UL1TR000124 for Yibin Wang. The NINDS Informatics Center for Neurogenetics and Neurogenomics (P30 NS062691) for Giovanni Coppola and Fuying Gao.

References

1. Finnemore A, Groves A. Physiology of the fetal and transitional circulation. Semin Fetal Neonatal Med. 2015; 20:210–216. [PubMed: 25921445]
2. Donn MS. Fetal-to-neonatal maladaptation. Semin Fetal Neonatal Med. 2006; 11:166–173. [PubMed: 16564756]
3. Porrello ER, Mohmoud AI, Simpson E, Hill JA, Richardson JA, Olson EN, et al. Transient regenerative potential of the neonatal mouse heart. Science. 2011; 331:1078–1080. [PubMed: 21350179]

4. Harvey RP. Patterning the vertebrate heart. Nat Rev Genet. 2002; 3:544–556. [PubMed: 12094232]
5. Srivastava D. Making or breaking the heart: from lineage determination to morphogenesis. Cell. 2006b; 126:1037–1048. [PubMed: 16990131]
6. Vincent SD, Buckingham ME. How to make a heart: the origin and regulation of cardiac progenitor cells. Curr Top Dev Biol. 2010; 90:1–41. [PubMed: 20691846]
7. Olson EN. Gene regulatory networks in the evolution and development of the heart. Science. 2006; 313:1922–1927. [PubMed: 17008524]
8. McCulley DJ, Black BL. Transcription factor pathways and congenital heart disease. Curr Top Dev Biol. 2012; 100:253–277. [PubMed: 22449847]
9. Bruneau BG. The developmental genetics of congenital heart disease. Nature. 2008; 451:943–948. [PubMed: 18288184]
10. Laflamme MA, Murry CE. Heart regeneration. Nature. 2011; 473:326–335. [PubMed: 21593865]
11. Fishman NH, Hof RB, Roudolph AM. Models of congenital heart disease in fetal lamb. Circulation. 1978; 58:354–364. [PubMed: 668085]
12. Gan J, Sonntag HJ, Tang MK, Cai D, Lee KK. Integrative Analysis of the Developing Postnatal Mouse Heart Transcriptome. PLoS ONE. 2015; 10:e0133288. [PubMed: 26200114]
13. Gong G, Song M, Csordas G, Kelly DP, Matkovich SJ, Dorn GW II. Parkin-mediated mitophagy directs perinatal cardiac metabolic maturation in mice. Science. 2015; 350:aad2459. [PubMed: 26785495]
14. Lee JH, Chen G, Peng G, Greer C, Ren R, Wang Y, et al. Analysis of Transcriptome Complexity through RNA Sequencing in Normal and Failing Murine Hearts. Circ Res. 2011; 109:1332–1341. [PubMed: 22034492]
15. Yang KC, Yamada KA, Patel AY, Topkara VK, George I, Cheema FH, et al. Deep RNA Sequencing Reveals Dynamic Regulation of Myocardial Noncoding RNA in Failing Human Heart and Remodeling with Mechanical Circulatory Support. Circulation. 2014; 129:1009–1021. [PubMed: 24429688]
16. Mercer TR, Dinger ME, Mattick JS. Long non-coding RNAs: insights into functions. Nat Rev Genet. 2009; 10:155–159. [PubMed: 19188922]
17. Mercer TR, Mattick JS. Structure and function of long noncoding RNAs in epigenetic regulation. Nat Struct Mol Biol. 2013; 20:300–307. [PubMed: 23463315]
18. Matkovich SJ, Edwards JR, Grossenheider TC, Strong CG, Dorn GW II. Epigenetic coordination of embryonic heart transcription by dynamically regulated long noncoding RNAs. Proc Natl Acad Sci USA. 2014; 111:12264–12269. [PubMed: 25071214]
19. He C, Hu H, Wilson KD, Wu H, Feng J, Xia S, et al. Systematic Characterization of Long Noncoding RNAs Reveals the Contrasting Coordination of Cis- and Trans-Molecular Regulation in Human Fetal and Adult Hearts. Circ Cardiovasc Genet. 2016; 9:110–118. [PubMed: 26896382]
20. Ritter O, Haase H, Schulte HD, Lange PE, Morano I. Remodeling of the hypertrophied human myocardium by cardiac bHLH transcription factors. J Cell Biochem. 1999; 74:551–561. [PubMed: 10440925]
21. Rinn JL, Kertesz M, Wang JK, Squazzo SL, Xu X, Brugmann SA, et al. Functional demarcation of active and silent chromatin domains in human HOX loci by noncoding RNAs. Cell. 2007; 129:1311–1323. [PubMed: 17604720]
22. Mercer TR, Mattick JS. Structure and function of long noncoding RNAs in epigenetic regulation. Nat Struct Mol Biol. 2013; 20:300–307. [PubMed: 23463315]
23. Wang X, Arai S, Song X, Reichart D, Du K, Pascual G, et al. Induced ncRNAs allosterically modify RNA-binding proteins in cis to inhibit transcription. Nature. 2008; 454:126–130. [PubMed: 18509338]
24. Martianov I, Ramadass A, Serra Barros A, Chow N, Akoulitchev A. Repression of the human dihydrofolate reductase gene by a non-coding interfering transcript. Nature. 2007; 445:666–670. [PubMed: 17237763]
25. Kurian L, Aguirre A, Sancho-Martinez I, Benner C, Hishida T, Nguyen TB, et al. Identification of novel long noncoding RNAs underlying vertebrate cardiovascular development. Circulation. 2015; 131:1278–1290. [PubMed: 25739401]

26. Grote P, Wittler L, Hendrix D, Koch F, Wahrisch S, Beisaw A, et al. The tissue-specific lncRNA Fendrr is an essential regulator of heart and body wall development in the mouse. Dev Cell. 2013; 24:206–214. [PubMed: 23369715]
27. Klattenhoff CA, Scheuermann JC, Surface LE, Bradley RK, Fields PA, Steinhauser ML, et al. Braveheart, a long noncoding RNA required for cardiovascular lineage commitment. Cell. 2013; 152:570–583. [PubMed: 23352431]
28. Han P, Li W, Lin CH, Yang J, Shang C, Nurnberg ST, et al. A long noncoding RNA protects the heart from pathological hypertrophy. Nature. 2014; 514:102–106. [PubMed: 25119045]
29. Ishii N, Ozaki K, Sato H, Mizuno H, Saito S, Takahashi A, et al. Identification of a novel non-coding RNA, MIAT that confers risk of myocardial infarction. J Hum Genet. 2006; 51:1087–1099. [PubMed: 17066261]
30. Sun K, Chen X, Jiang P, Song X, Wang H, Sun H. iSeeRNA: identification of long intergenic non-coding RNA transcripts from transcriptome sequencing data. BMC Genomics. 2013; 14(Suppl 2):S7.
31. Langfelder P, Horvath S. WGCNA: an R package for weighted correlation network analysis. BMC Bioinformatics. 2008; 9:559. [PubMed: 19114008]
32. Hu G, Chen J. A genome-wide regulatory network identifies key transcription factors for memory CD8+ T-cell development. Nat Commun. 2013; 4:2830. [PubMed: 24335726]
33. Ya J, Schilham MW, de Boer PA, Moorman AF, Clevers H, Lamers WH. Sox4-deficiency syndrome in mice is an animal model for common trunk. Circ Res. 1998; 83:986–994. [PubMed: 9815146]
34. Penzo-Méndez A, Dy P, Pallavi B, Lefebvre V. Generation of Mice Harboring a Sox4 Conditional Null Allele. Genesis. 2007; 45:776–778. [PubMed: 18064674]
35. Markert CD, Ning J, Staley JT, Heinzke L, Childers CK, Ferreira JA, et al. TCAP knockdown by RNA interference inhibits myoblast differentiation in cultured skeletal muscle cells. Neuromuscul Disord. 2008; 18:413–422. [PubMed: 18440815]
36. Zhang R, Yang J, Zhu J, Xu X. Depletion of zebrafish Tcap leads to muscular dystrophy via disrupting sarcomere-membrane interaction, not sarcomere assembly. Hum Mol Genet. 2009; 18:4130–4170. [PubMed: 19679566]
37. Lange S, Himmel M, Auerbach D, Agarkova I, Hayess K, Furst DO, et al. Dimerization of Myomesin: Implications for the Structure of the Sarcomeric M-band. J Mol Biol. 2005; 345:289–298. [PubMed: 15571722]
38. Alloush J, Roof SR, Beck EX, Ziolo MT, Weisleder N. Expression levels of sarcolemmal membrane repair proteins following prolonged exercise training in mice. Indian J Biochem Biophys. 2013; 50:428–435. [PubMed: 24772964]
39. Schurch NJ, Schofield P, Gierliński M, Cole C, Sherstnev A, Singh V, et al. How many biological replicates are needed in an RNA-seq experiment and which differential expression tool should you use? RNA. 2016; 22:839–851. [PubMed: 27022035]
40. Nelson BR, Anderson DM, Olson EN. Small Open Reading Frames Pack a Big Punch in Cardiac Calcium Regulation. Circ Res. 2014; 114:18–20. [PubMed: 24385504]
41. Nelson BR, Makarewich CA, Anderson DM, Winders BR, Troupes CD, Wu FA. A peptide encoded by a transcript annotated as long noncoding RNA enhances SERCA activity in muscle. Science. 2016; 351:271–275. [PubMed: 26816378]

Clinical Perspective

Collectively phrased as “perinatal circulatory transition”, fetal to neonatal transition of the heart is a complex but tightly regulated process. Its perturbation may have major implications in congenital heart defects (CHDs) and failure of the premature heart. Transcriptome programming is the driving force for functional adaptation and maturation of the heart. However, our current understanding of transcriptome changes in neonatal heart chambers, in particular involving long noncoding (lnc) RNA species, is limited. Here we undertook a multi-layered and integrated systems analysis of neonatal heart transcriptome at three time points of perinatal circulatory transition. We find that transcriptome changes, including both protein coding RNAs and lncRNAs, are more significantly driven by developmental stage than ventricular chamber specificity. Chamber specific and developmental stage specific lncRNA/mRNA gene networks are identified to be associated with dynamic changes in myocyte proliferation and maturation. Novel interactions between mRNA and lncRNA species are revealed with potentially significant impact on myocyte function. The result of this study will help dissect the molecular mechanisms involved in perinatal circulatory transition in heart and facilitate the discovery of potential diagnostic and therapeutic targets for congenital heart defects and failure of the premature heart.

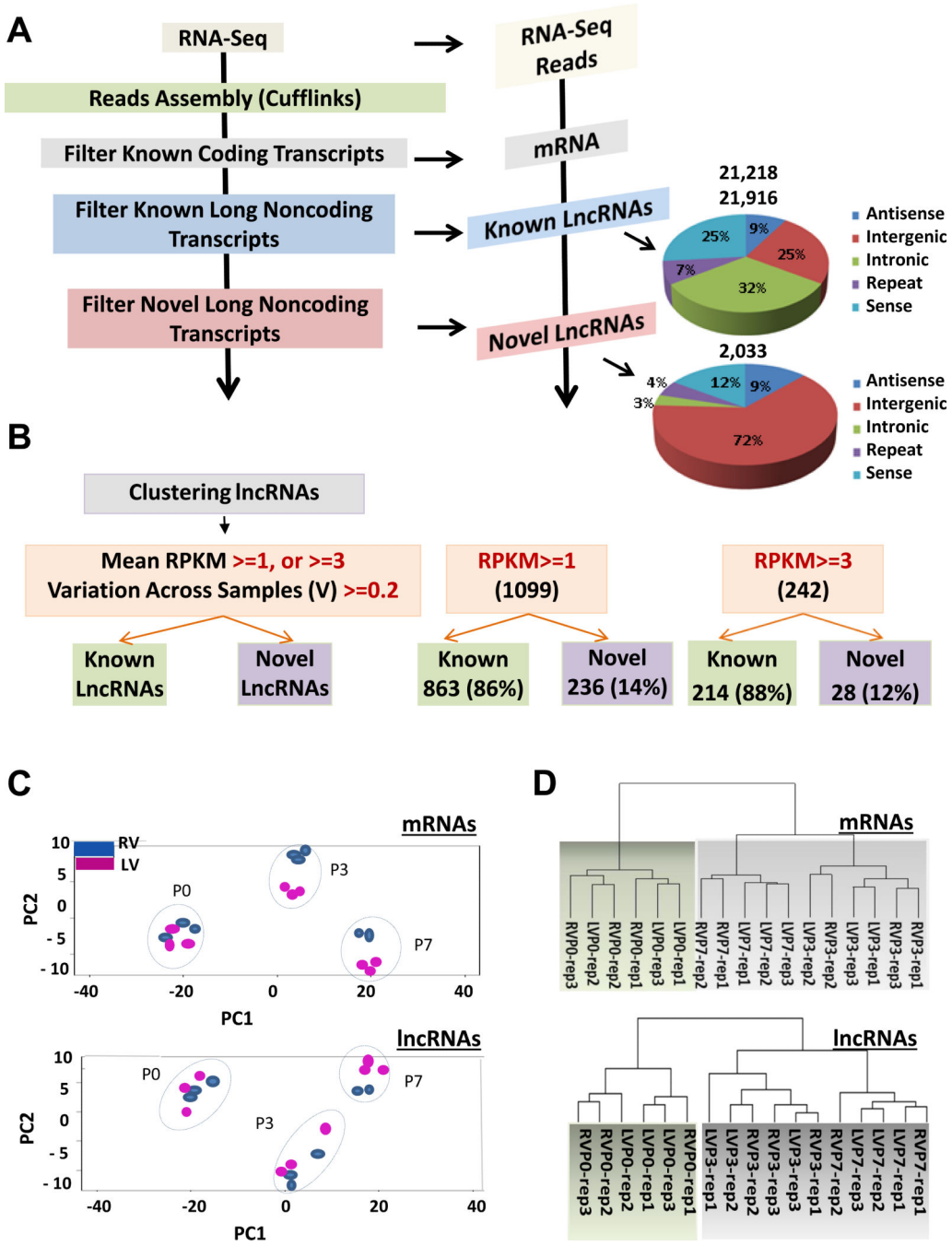

Figure 1.

Transcriptome Landscape in Neonatal Mouse Heart Chambers. **A.** Schematic representation of bioinformatics pipeline and expression statistics of mapped RNA transcripts (absolute numbers of detected genes and lncRNAs are shown). Pie charts represent percentage of neonatal heart lncRNA sub-classes. **B.** Schematic representation of lncRNA clustering analysis algorithm. Numbers of known versus novel lncRNAs using different expression cutoff values are shown. **C.** Principal component analysis (PCA) of top 500 varying mRNAs *(upper panel)* and lncRNAs *(lower panel)* across maturation stages. **D.** Unsupervised

hierarchical clustering of mRNAs *(upper panel)* and lncRNAs *(lower panel)* derived from 17 RNA-Seq samples.

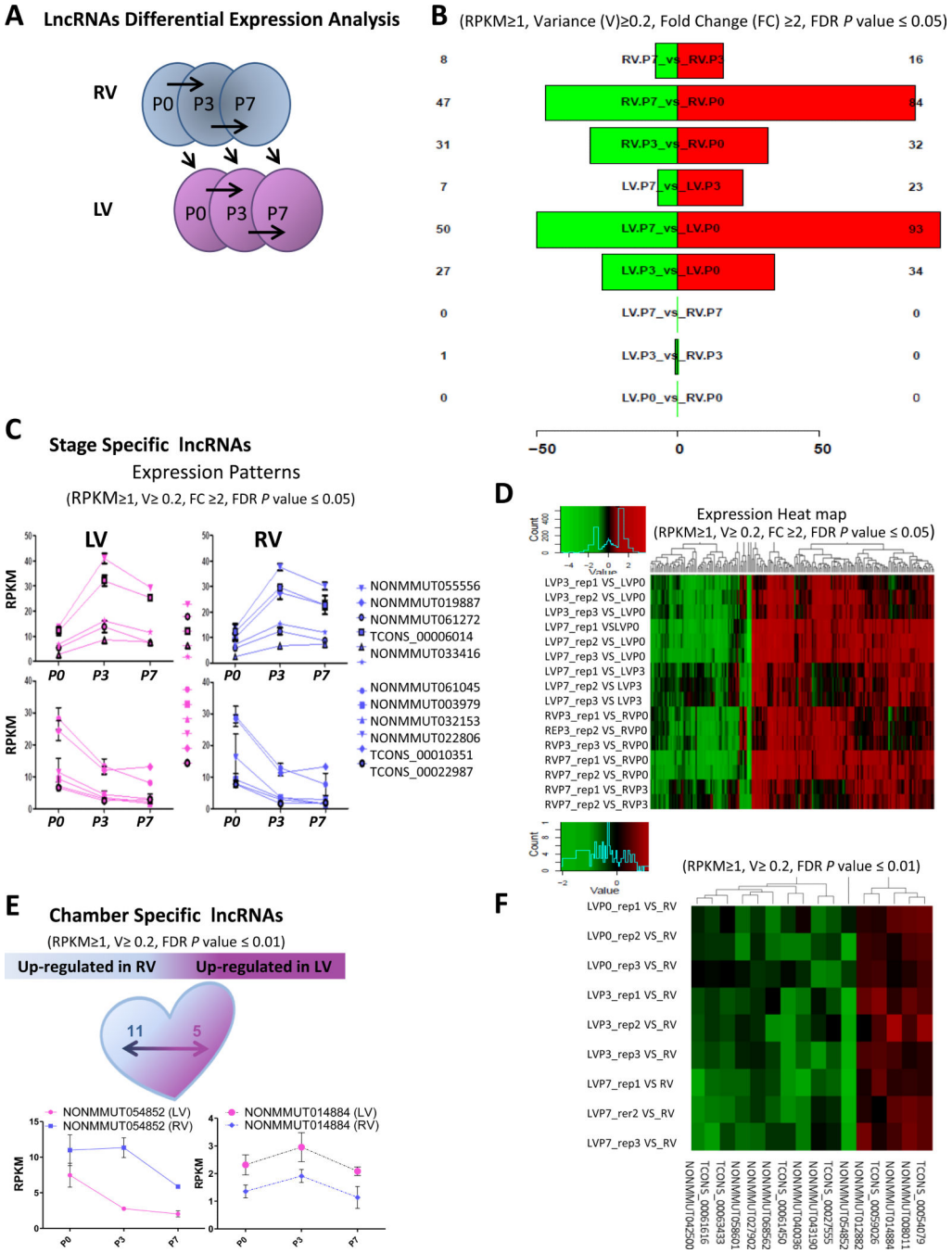

Figure 2.

LncRNAs are Dynamically Regulated in Neonatal Heart along Maturation Stages. **A.** Schematic representation of pair wise comparative (differential expression) analysis along 2 schemes: stage specific and chamber specific. **B.** Numbers of significantly differentially expressed lncRNAs (cutoff values: RPKM>=1, V>=0.2, FDR *P*<= 0.05, FC >=2) in stage specific and chamber specific comparisons. (Red: Upregulated, Green: Downregulated) **C.** Expression time course and patterns of representative stage specific lncRNAs in LV (left ventricle/pink) and RV (right ventricle/blue). **D.** Expression heat maps (Z score) of stage

specific differentially expressed lncRNAs in LV and RV. Columns represent lncRNAs and rows represent expression ratio between developmental stages being compared. (Red: Upregulated, Green: Downregulated) **E.** Chamber specific lncRNAs and representative expression time courses showing chamber specific divergence (cutoff values RPKM>=1, V>=0.2, FDR *P*<=0.01). **F.** Expression heat maps (Z score) of chamber specific differentially expressed lncRNAs in LV in contrast to RV overall. Columns represent lncRNAs and rows represent expression ratio of each LV sample in contrast to RV. (Red: Upregulated, Green: Downregulated).

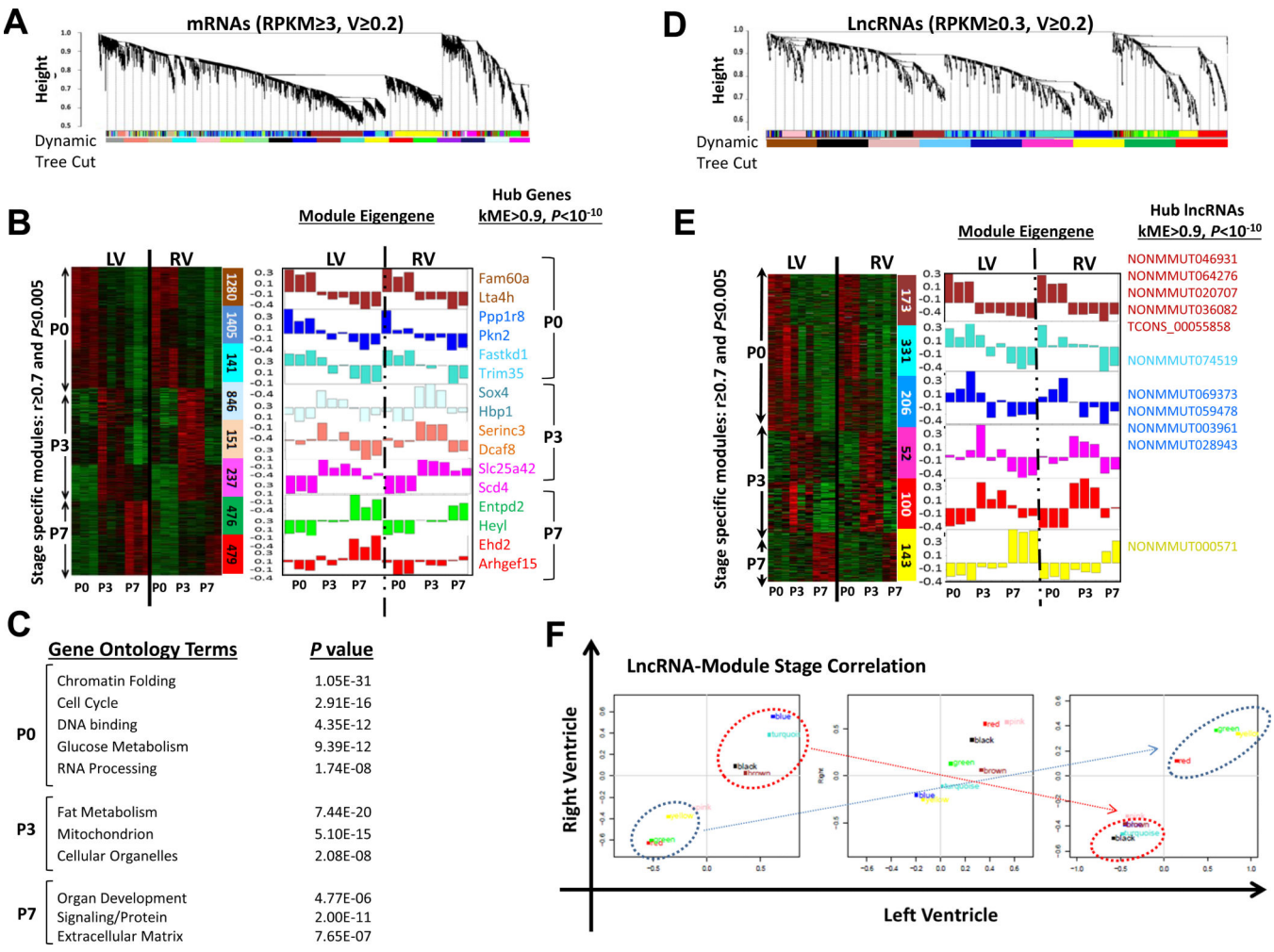

Figure 3.

Weighted Gene Co-expression Network Analysis (WGCNA) Revealed Stage Specific mRNA and lncRNA Module Gene Network in Neonatal Heart. **A. D.** WGCNA dendrograms of protein coding mRNAs (A) and lncRNAs (D) expression reveal different expression modules. Branches in the hierarchical clustering dendrograms correspond to modules. Color-coded module membership is displayed in the color bars below the dendrograms. Y axes (height) represent module significance (correlation with external trait). **B.** Heat map depicting expression profiles of stage specific mRNA modules member genes. Eight stage specific modules overlapping in LV and RV and numbers of genes corresponding to each module are shown (color-bars). Eigengene expression of a given module is presented (bar graphs) along with representative top two correlated hub genes for each module. The expression profiles are standardized. Red and green correspond to high and low expression values, respectively. Intramodular gene connectivity measure (kME) >0.9 and $P<10^{-10}$ are required to identify hub genes. Module-stage correlation cutoff values r≥0.7 and $P\leq0.005$ are required. (r. Pearson's correlation coefficient; *P. P* value). Color code of the modules is preserved. **C.** Top Gene Ontology (GO) terms enriched in corresponding stage specific modules are listed with their *P* values. **E.** Heat map depicting expression profiles of stage specific lncRNA module members. Six stage specific modules overlapping in LV and RV

and numbers of corresponding lncRNA members are shown (color-bars). Eigengene expression of a given module is presented (bar graphs). Correlated hub-lncRNAs for each stage specific module are also presented. Color code of the modules is preserved. **F.** Correlation plots depicting lncRNA modules correlation with LV trait (X Axis) and RV trait (Y Axis) at P0, P3, and P7.

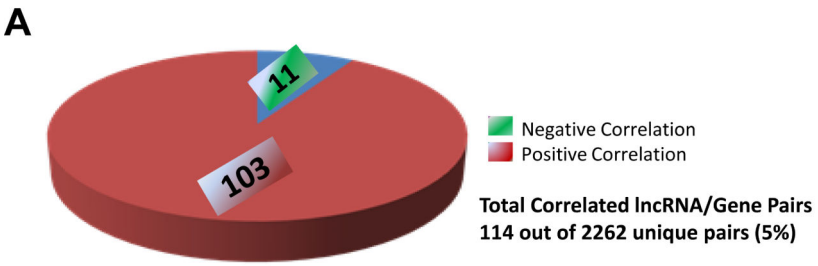

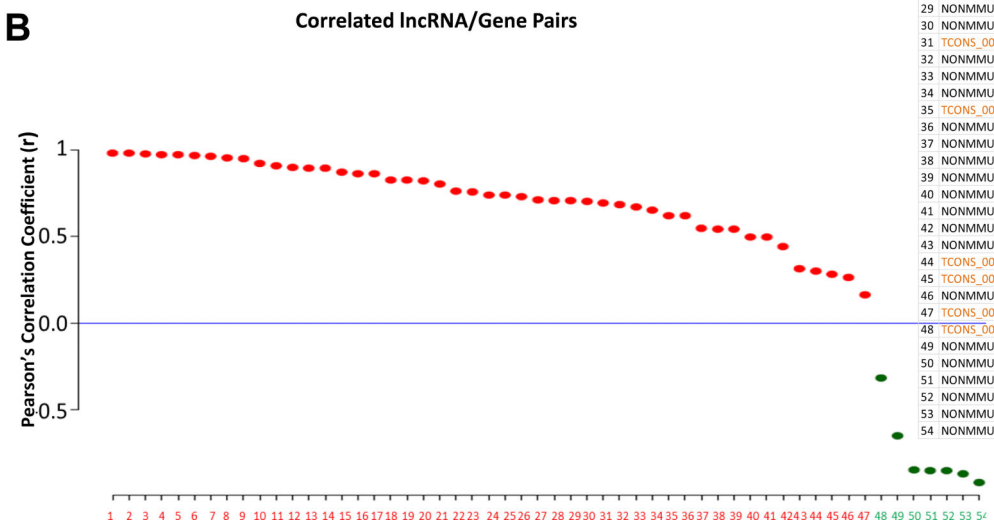

C

#	LncRNA	Gene (Ensemble)	r (Pearson's)	BH-Add. *P* value
1	NONMMUT062940	Ucp3	0.980650378	1.18E-08
2	NONMMUT041263	Kcnb1	0.979889166	1.57E-08
3	NONMMUT030790	Slc8a1	0.978479667	2.60E-08
4	NONMMUT030790	Vash1	0.974092768	1.03E-07
5	NONMMUT069029	Ncam1	0.97277105	1.49E-07
6	NONMMUT015781	Gm24895	0.967030796	6.16E-07
7	NONMMUT028256	Gm16574	0.96432598	1.10E-06
8	NONMMUT073984	Tceal8	0.95497753	6.16E-06
9	NONMMUT045557	Gbp3	0.951041042	1.14E-05
10	NONMMUT042746	Hspa4l	0.9196209	2.32E-06
11	TCONS_00034921	Fastkd1	0.9080328	4.61E-06
12	NONMMUT028254	Igf2r	0.9006681	1.52E-05
13	NONMMUT049523	Zmym6	0.8940063	1.52E-05
14	NONMMUT066751	Nudt21	0.8922454	1.52E-05
15	TCONS_00007592	Slit3	0.8694928	3.97E-05
16	NONMMUT039323	Rad51	0.8600282	5.60E-05
17	NONMMUT012867	Jmjd6	0.858928181	7.64E-04
18	NONMMUT020640	Mapk1ip1l	0.8277763	1.68E-04
19	NONMMUT068830	Mcam	0.8243618	1.83E-04
20	TCONS_00026073	Nkx2-5	0.8188352	2.17E-04
21	NONMMUT021062	Xpo4	0.8022637	3.37E-04
22	NONMMUT071345	Ctdspl	0.7634787	9.90E-04
23	TCONS_00020576	Hnrnpa1	0.7565583	9.53E-04
24	TCONS_00026074	Nkx2-5	0.7368761	1.79E-03
25	NONMMUT055686	C1galt1	0.7367618	1.79E-03
26	NONMMUT011579	Luc7l3	0.7288156	2.06E-03
27	NONMMUT034568	Pcgf5	0.713185	2.73E-03
28	TCONS_00020303	Shank3	0.7067435	2.88E-03
29	NONMMUT065691	Hand2	0.7046582	2.88E-03
30	NONMMUT023874	Ago2	0.7037665	2.88E-03
31	TCONS_00003436	Soat1	0.6940464	3.41E-03
32	NONMMUT035170	Nhlrc2	0.6849452	3.96E-03
33	NONMMUT045460	H2afz	0.6713575	5.00E-03
34	NONMMUT012009	Klhl11	0.6528193	6.83E-03
35	TCONS_00008829	Kpnb1	0.6214237	1.10E-02
36	NONMMUT022720	Lmbrd2	0.6201133	1.16E-02
37	NONMMUT059324	Pde3a	0.5478524	3.04E-02
38	NONMMUT011437	Msi2	0.5438869	3.28E-02
39	NONMMUT068830	Cbl	0.5397882	3.35E-02
40	NONMMUT046193	Dpy19l4	0.4977373	4.97E-02
41	NONMMUT025170	Smug1	0.4967273	5.07E-02
42	NONMMUT033516	Rbm14	0.4394524	9.09E-02
43	NONMMUT003017	Cdc73	0.3119008	2.47E-01
44	TCONS_00006555	Mex3d	0.2997066	2.62E-01
45	TCONS_00029263	Ppp1r14b	0.2828418	2.85E-01
46	NONMMUT013008	Cdon	0.2632908	3.07E-01
47	TCONS_00026340	Bag6	0.1604652	5.53E-01
48	TCONS_00028943	Acaa2	-0.3161513	2.46E-01
49	NONMMUT061272	Nol10	-0.651945	6.86E-03
50	NONMMUT063779	Trim72	-0.848040957	0.041015684
51	NONMMUT011874	Tcap	-0.853393886	0.031859237
52	NONMMUT033633	Frmd8	-0.853645061	0.031476221
53	NONMMUT070831	Twf2	-0.871927021	0.012231025
54	NONMMUT010464	Acadvl	-0.920302966	0.000402941

Figure 4.

LncRNAs Correlation with Neighboring Genes. **A.** Pie chart showing the numbers of collocated lncRNA/mRNA pairs with significant expression correlation in at least one developmental stage (r≥0.9, B-H adjusted Pearson's *P* value≤0.05). **B.** Correlation plot of representative significantly correlated lncRNA/mRNA pairs depicting positive and negative expression correlation relationship. **C.** List of the correlated lncRNA/gene pairs. Novel lncRNAs are labeled in orange. (A complete list of significantly correlated lncRNA/mRNA pairs is presented in Supplemental Table 5) (BH: Benjamini-Hochberg; r: Pearson's correlation coefficient; *P: P* value).

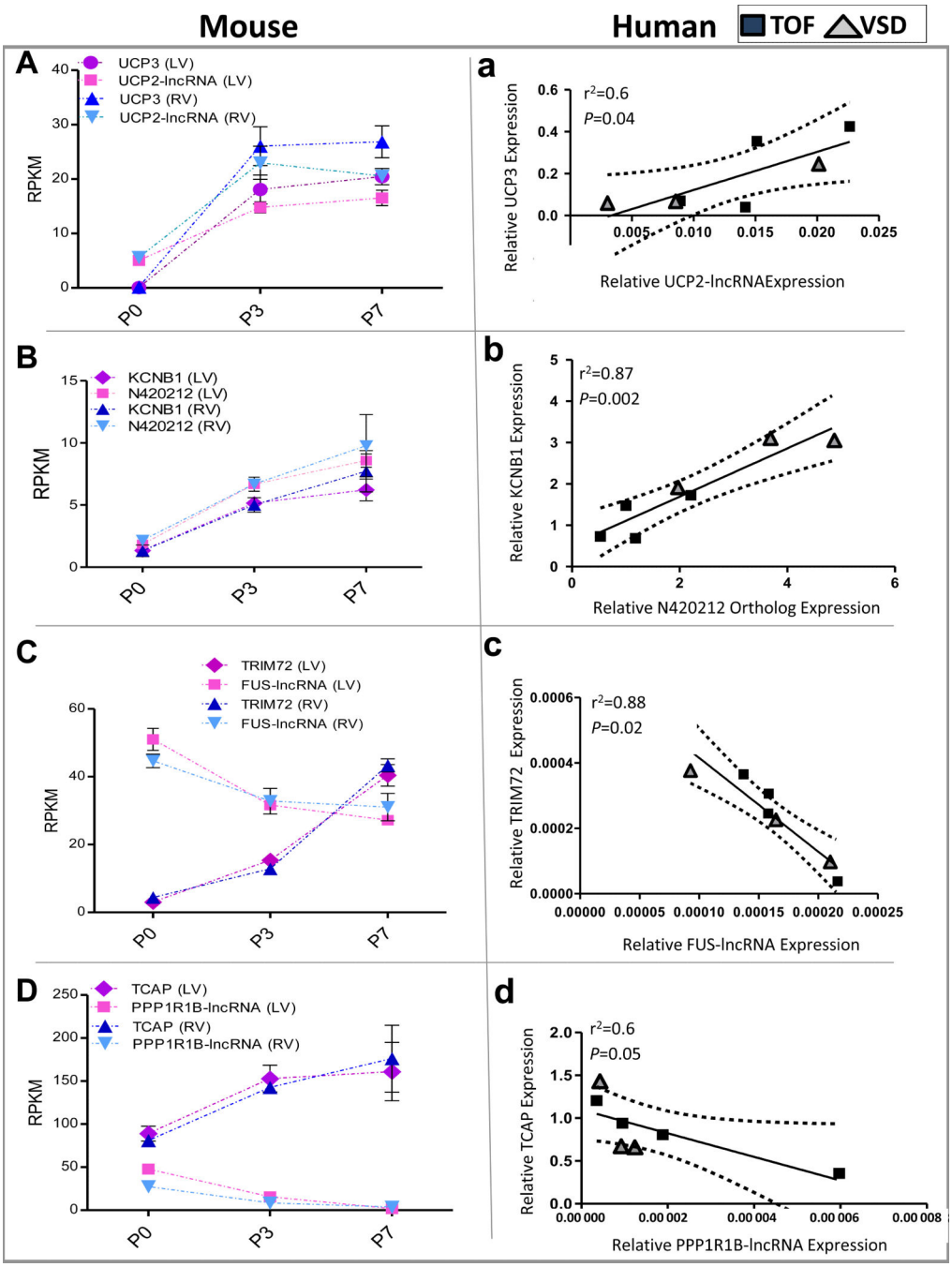

Figure 5.

Conserved Expression Correlation Relationship Between lncRNA/mRNA Partners in Human Infantile Heart. **A. B. C. D.** Expression time courses (RNA-seq) of lncRNAs (Ucp2-lncRNA, n420212, FUS-lncRNA and Ppp1r1b-lncRNA) in LV (light pink) and RV (light blue) and partner mRNAs (Ucp3, Kcnb1, Trim72 and Tcap, respectively) in LV (dark pink) and RV (dark blue). **a,b,c,d.** Correlation graphs depicting expression correlation relationship between lncRNAs (UCP2, NONMMUT041263, FUS-lncRNA and PPP1R1B-lncRNA) (X Axis) and partner mRNAs (UCP3, KCNB1, TRIM72 and TCAP, respectively) (Y Axis) in

human congenital heart defect (CHD) samples. (TOF: Tetralogy of Fallot; VSD: Ventricular Septal Defect; r: Pearson's correlation coefficient; *P: P* value). The dotted lines represent the 25% confidence intervals. Age of the patients ranged between 2-24 m/o for TOF cases (n=4), and between 2-5 y/o for VSD cases (n=3).

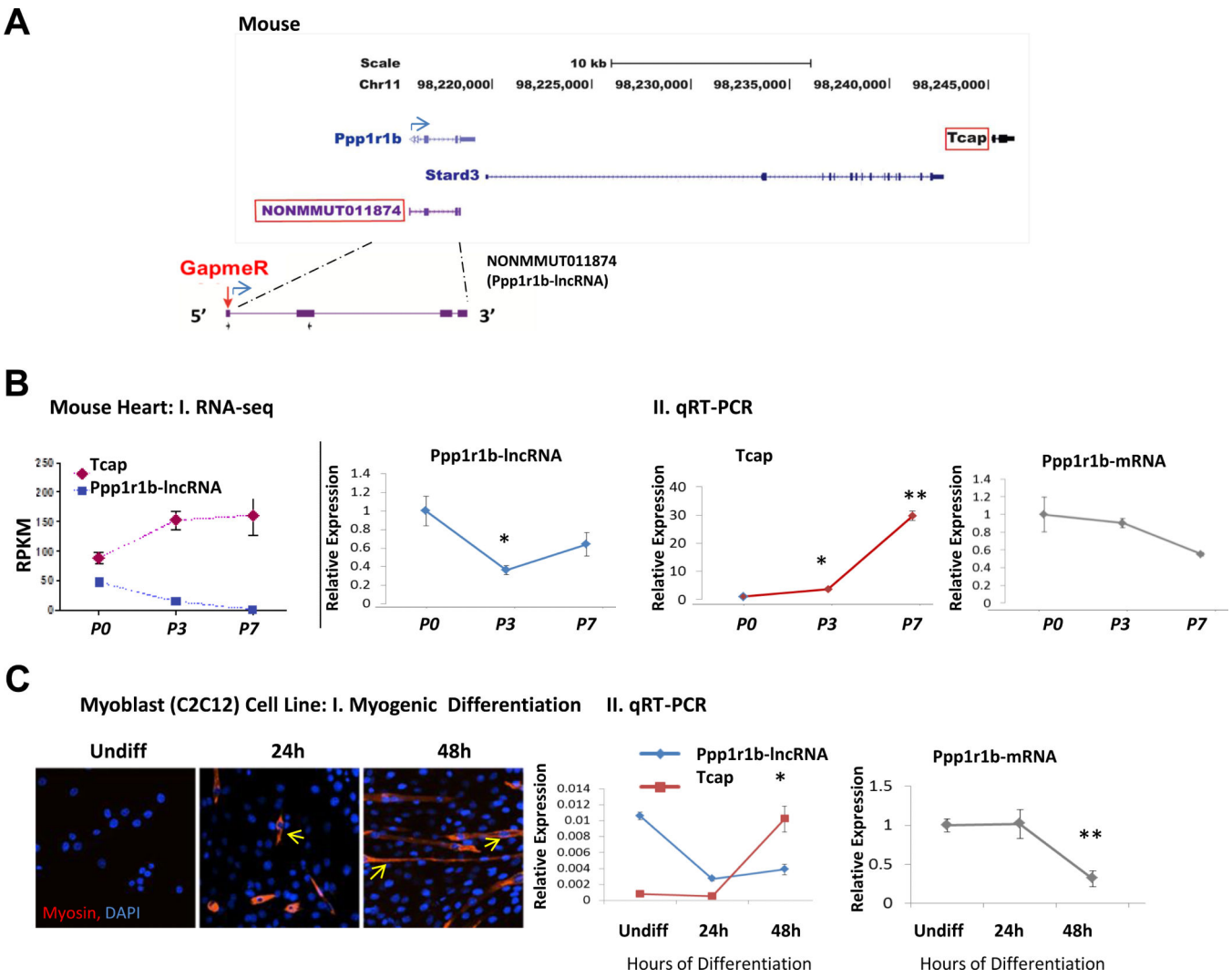

Figure 6.

Ppp1r1b-lncRNA (NONMMUT011874) and Tcap are Inversely Regulated in Neonatal Mouse Heart and in C2C12 Cell Line. **A.** Genomic position of mouse Ppp1r1b-lncRNA in relation to Tcap on mouse Chromosome 11 and schematic representation of GapmeR (antisense Oligo) targeting site. **B.** Quantitative validation (qRT-PCR) of Ppp1r1b-lncRNA, Tcap, and Ppp1r1b-mRNA expression time course in neonatal mouse heart (I. RNA-seq data, II. qRT-PCR data). **C**. Quantitative validation of Ppp1r1b-lncRNA, Tcap, and Ppp1r1b-mRNA expression time course during myoblast differentiation. I: Confocal images depicting differentiation time course of cultured mouse myoblast cell line (C2C12). Yellow arrows indicate myosin positive multinucleated myotubes. II: Expression time course (qRT-PCR) of Ppp1r1b-lncRNA, Tcap, and Ppp1r1b-mRNA during C2C12 differentiation (n= 3 replicates).

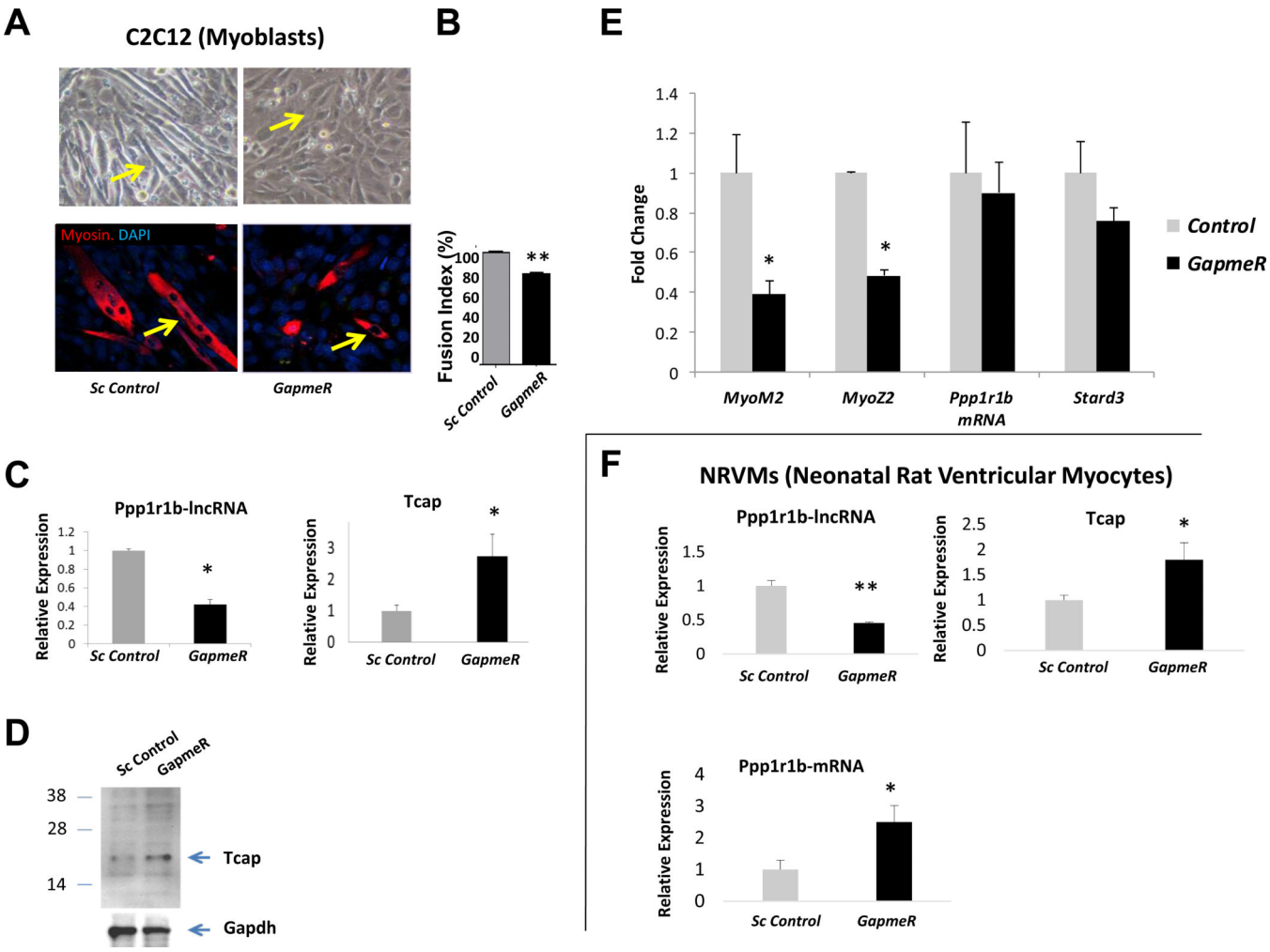

Figure 7.

Ppp1r1b-lncRNA (NONMMUT011874) Regulates Tcap Expression and Myogenesis in Cultured C2C12 Myoblast Cell Line. **A.** Light microscopy (*upper*) and confocal images of cultured C2C12 cells in response to GapmeR compared to scrambled control. **B.** Semi-quantitative analysis of myogenic differentiation using fusion index. **C, E**. Quantitative expression of Ppp1r1b-lncRNA, Tcap, Myoz2, Myom2, Ppp1r1b and Stard3 in C2C12 cells in response to GapmeR compared to scrambled control 48 hours post treatment. **D.** Increased Tcap protein abundance in response to Ppp1r1b-lncRNA knockdown. **F.** Quantitative expression of Ppp1r1b-lncRNA, Tcap, and Ppp1r1b-mRNA in neonatal rat ventricular myocytes (NRVMs) in response to GapmeR compared to scrambled control. (n=3 replicates per condition).

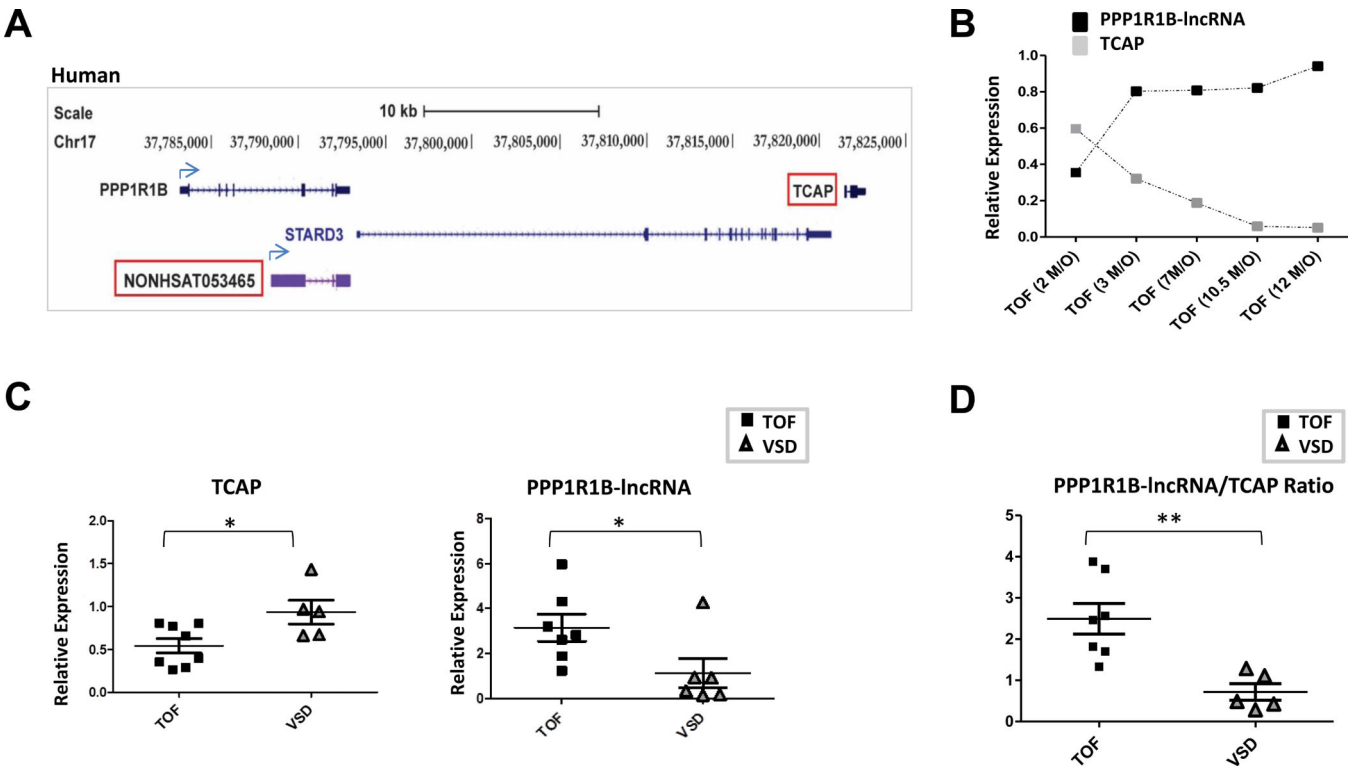

Figure 8.

PPP1R1B-lncRNA/TCAP Expression Ratio Segregates Human Congenital Heart Defect Phenotypes. **A.** Genomic position of human PPP1R1B-lncRNA ortholog (annotated as NONHSAT053465) on chromosome 17. **B.** Expression time course of PPP1R1B-lncRNA and TCAP in human infantile hearts with TOF (n= 5). **C.** PPP1R1B-lncRNA and TCAP are inversely regulated in TOF vs VSD patients. **D.** PPP1R1B-lncRNA/TCAP ratio significantly segregates with disease phenotype (TOF vs VSD). (TOF: n=8, age range: 2-24 m/o; VSD: n=6, age range: 2-5y/o.), PPP1R1B-lncRNA didn't amplify in one VSD sample, and TCAP didn't amplify in one TOF sample. Those two samples were therefore excluded. The remaining samples were used for PPP1R1B-lncRNA/TCAP ratio.